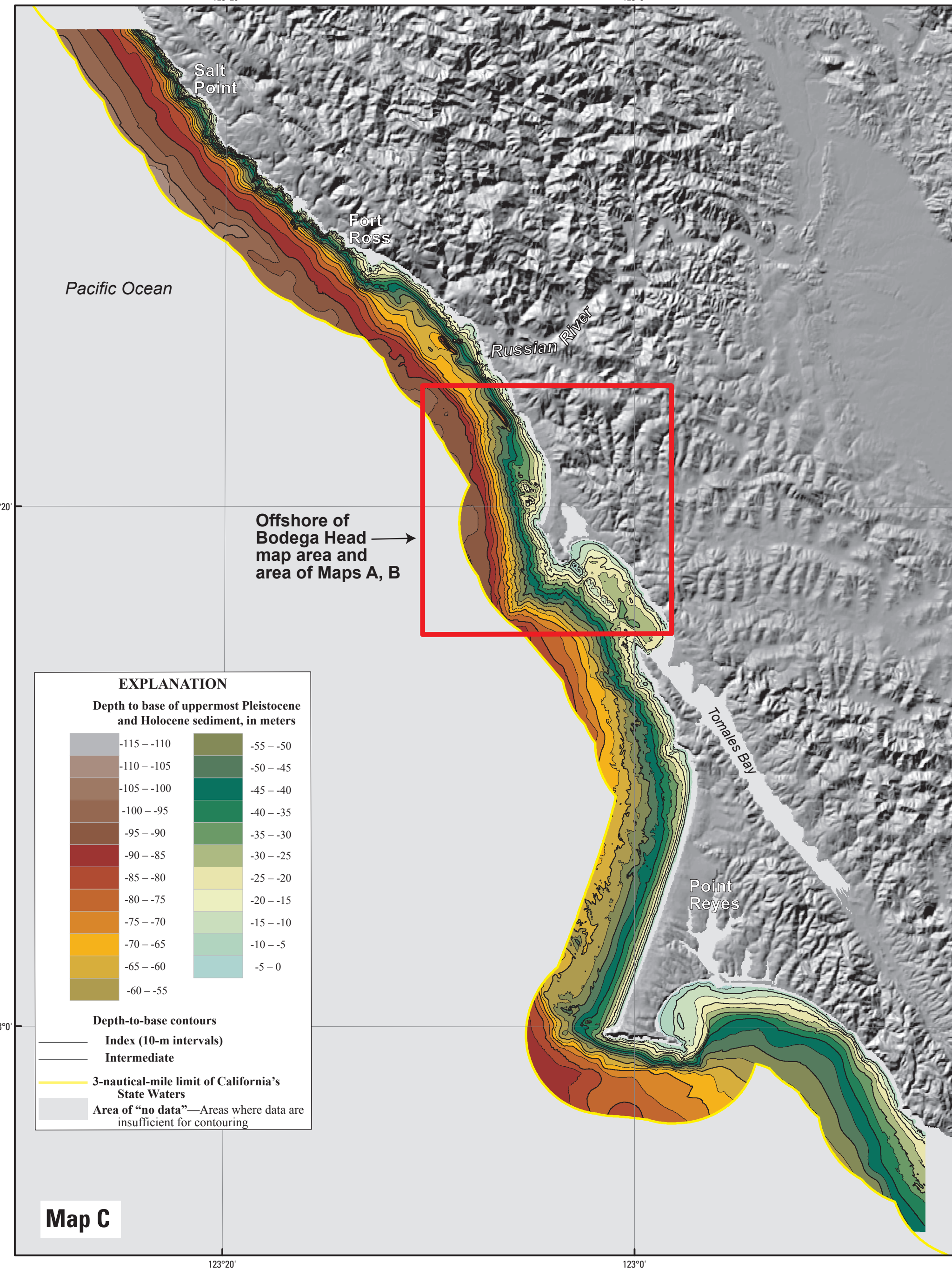


Figure 1. USGS high-resolution minispar seismic-reflection profile PR-102 collected in 2009 on survey S-8-09-NCI which crosses shelf west-southwest of Duncan's Point (see Map A for location; see also, fig. 1 on sheet 8). Profile shows San Andreas Fault Zone and gently dipping strata west of zone beneath nearshore and continental shelf (see Map A for location; also shown on sheet 8, fig. 11). Dashed red lines show faults. Blue shading shows inferred uppermost Pleistocene and Holocene shelf strata, deposited since last sea-level lowstand about 21,000 years ago. Dashed purple line shows erosional unconformity between inferred Quaternary strata and reflection-free bedrock (probably the granitic rocks of Bodega Head). Dashed green lines highlight continuous reflections that illustrate gentle dip and low-angle bedding of strata. Dashed yellow line is seaward multiple tectonic offshore reflector. Purple triangle shows location of California's State Waters limit (yellow line on Maps A, B, C, D, E).

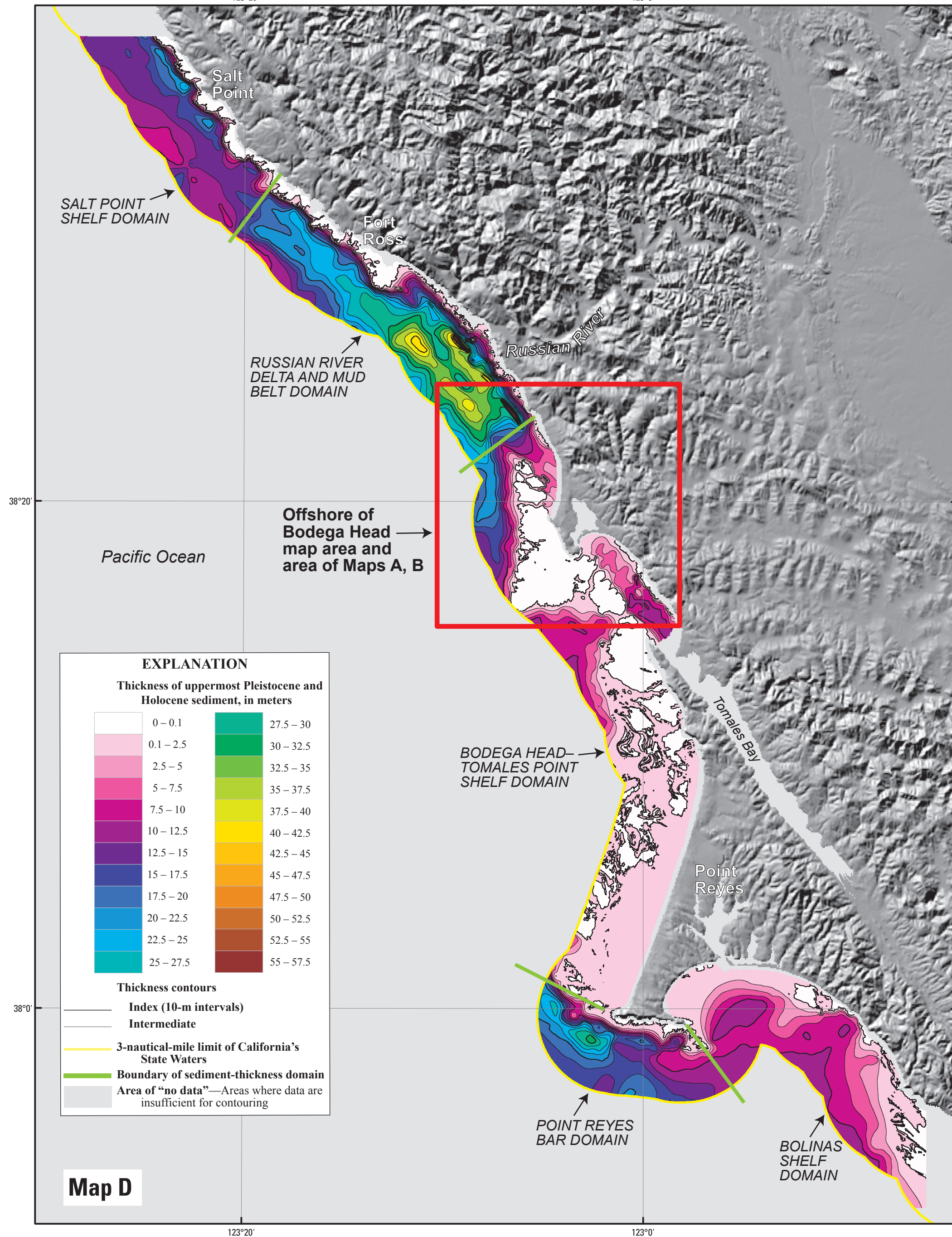
Map A
Depth and thickness mapped by Samuel Y. Johnson and Stephen R. Hartwell, 2011-2012.
GIS database and digital cartography by Stephen R. Hartwell.

Map B
Depth and thickness mapped by Samuel Y. Johnson and Stephen R. Hartwell, 2011-2012.
GIS database and digital cartography by Stephen R. Hartwell.

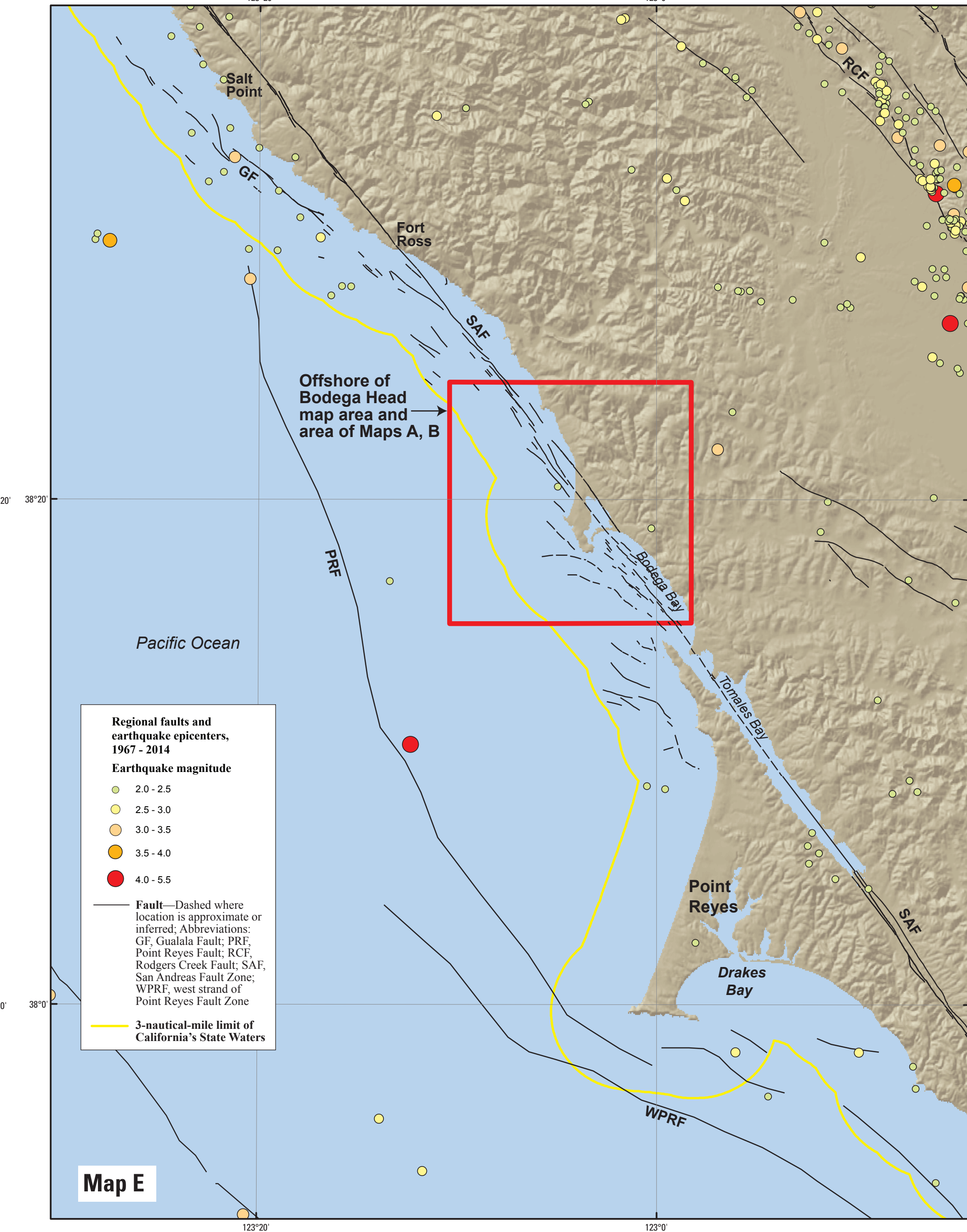
Map C
Depth and thickness mapped by Samuel Y. Johnson and Stephen R. Hartwell, 2011-2012.
GIS database and digital cartography by Stephen R. Hartwell.



Map C
Depth and thickness mapped by Samuel Y. Johnson and Stephen R. Hartwell, 2011-2012.
GIS database and digital cartography by Stephen R. Hartwell.



Map D
Depth and thickness mapped by Samuel Y. Johnson and Stephen R. Hartwell, 2011-2012.
GIS database and digital cartography by Stephen R. Hartwell.



Map E
Depth and thickness mapped by Samuel Y. Johnson and Stephen R. Hartwell, 2011-2012.
GIS database and digital cartography by Stephen R. Hartwell.

DISCUSSION

This sheet includes maps that show the interpreted thickness and depth to base of uppermost Pleistocene and Holocene deposits in California's State Waters for the offshore of Bodega Head map area (Maps A, B), as well as for a larger area that extends along the coast about 115 km from Salt Point to Drakes Bay on the south flank of the Point Reyes peninsula (Maps C, D, E). To establish regional context, this uppermost stratigraphic unit (blue shading in seismic-reflection profile of fig. 1; see also, figs. 1, 2, 3, 4, 6, 7, 8, 9, 10, 11 on sheet 8) is inferred to have been deposited during the post-LGM sea-level rise in the last about 21,000 years (see, for example, Potter and Fairbanks, 2006; Stanford and others, 2011). The unit commonly is characterized either by "tonic transparency" or by parallel, low-amplitude, low- to high-frequency, continuous to moderately continuous, diffuse reflections (terminology from Mitchum and others, 1977). The contrast between this upper stratigraphic unit and underlying strata is a prominent, locally angular unconformity, inferred as a transgressive surface of erosion, commonly marked by channeling and a distinct upward change to lower amplitude, more diffuse reflections.

Offshore of Salt Point, about 25 km north of the offshore of Bodega Head map area, the sequence of uppermost Pleistocene and Holocene deposits, which lies above the prominent unconformity, includes a lower, older stratigraphic unit made up of a downlapping sediment wedge that formed along the southwest flank of nearshore bedrock outcrops. Stratigraphic position, depth of occurrence, and reflection geometry suggest that this lower unit formed during the latter stages of the pre-LGM sea-level fall (about 30,000 to 21,000 years ago). Our regional thickness and depth-to-base maps (Maps C, D) combine these two uppermost Pleistocene and Holocene units in this northern part of the Salt Point to Drakes Bay region.

To make these maps, water bottom and depth to base of the post-LGM horizons were mapped from seismic-reflection profiles (fig. 1; see also, sheet 8). The difference in the two horizons was exported for every 400 m as XY coordinates (UTM zone 10) and two-way travel time (TWT). The thickness of the post-LGM unit (Maps B, D) was determined by applying a sound velocity of 1,600 m/sec to the TWT. The thickness points were interpolated to a preliminary continuous surface, overlaid with zero-thickness bedrock outcrops (see sheet 10), and contoured, following the methodology of King and others (2012).

The thickness data points are dense along tracklines (about 1 m apart) and sparse between tracklines (1 km apart), resulting in minor contouring artifacts. To incorporate the effect of a few rapid thickness changes along faults, to remove irregularities through interpolation, and to reflect other geologic information and complexity, minor manual editing of the preliminary thickness contours was undertaken. Contour modifications and regrading were repeated several times to produce the final sediment-thickness maps. Information for the depth to base of the post-LGM unit (Maps A, C) was generated by adding the sediment-thickness data to water depths determined by multibeam bathymetry (see sheet 1).

The thickness of the post-LGM unit in the offshore of Bodega Head map area ranges from 0 to 56 m (Map B), and the depth to the base of the unit ranges from about 10 to 115 m (Map A). Mean sediment thickness for the map area is 9.9 m, and total sediment volume is 1,356 × 10⁹ m³. The thickest sediment is found in two areas in the northern part of the map area: (1) within a narrow (about 300 m wide), elongate (about 3 km long) sedimentary basin that formed in a subsiding, near-over setting within the San Andreas Fault Zone (fig. 1; see also, figs. 1, 2 on sheet 8), and (2) the western part of the Russian River delta and mud belt (see sheet 8, fig. 11). The mud belt lies offshore of the Russian River (Maps C, D), which occupies a large watershed (3,470 km²) and has a very large sediment load (estimated at 900,000 metric tons); Farnsworth and Warrick, 2007). The large thickness of sediment in this mudbelt area clearly is tied to the abundant sediment supply from this source. A paleochannel offshore of the much smaller Salinas Creek watershed (about 91 km²) also feeds the mudbelt zone from the southeast (Map B), and Salinas Creek is considered a secondary sediment source. Further south, much of the seaward west of Bodega Head is characterized either by outcrops of Cretaceous granitic basement rocks (see sheet 10) or by a thin to moderately thick (as much as 23 m) of relatively fine-grained sediment that overlies these basement rocks from the west (figs. 3, 9, 10 on sheet 8).

Bodega Bay straddles the San Andreas Fault Zone, which forms an about 2-km-wide linear basin bounded on the east by shallow outcrops of the Franciscan and Cretaceous Franciscan Complex and on the west by seaward outcrops of Cretaceous granitic rocks (see sheet 10). The sediment cover between the flanking basement terraces is relatively thin (0 to about 10 m) and has a complex, irregular distribution that is consistent with its location in an actively deforming fault zone. The isocham maps (Maps B, D) reveal an east-west-trending paleochannel that exists Bodega Bay in the southern part of the map area, which provided a sea-level-lowstand outlet for small, local coastal waterbodies and estuaries such as Tomales Bay, Estero Americano, and Estero de San Antonio (Maps A, B, C, D).

Five different "domains" of sediment thickness are recognized on the regional sediment-thickness map (Map D), each with distinctive geologic controls: (1) The Salt Point domain, located in the far northwestern part of the region, has a mean sediment thickness of 17.7 m. The thickest sediment (20 to 23 m) is found where a pre-LGM, regressive, downlapping sediment wedge formed above a break in slope that is controlled by a contact between harder bedrock and softer, folded Pleistocene strata. Sediment thinning in this domain within the outer parts of California's State Waters is the result of a relative lack of sediment supply from local waterbodies, as well as a more distal Russian River source; (2) The Russian River delta and mud belt domain, located offshore of the Russian River, the largest sediment source on this part of the coast, has the thickest uppermost Pleistocene and Holocene sediment in the region (mean thickness, 21.1 m). The northward extension into the mudbelt "mud belt" results from northward shelf-bottom currents and sediment transport (Drake and Cacchione, 1985). This domain includes a section of the San Andreas Fault Zone, which here is characterized by several releasing, right-stepping strands that bound narrow, elongate pull-apart basins; these sedimentary basins contain the greatest thickness of uppermost Pleistocene and Holocene sediment (about 56 m) in the region; (3) The Bodega Head-Tomales Point shelf domain, located between Bodega Head and the Point Reyes headland, contains the least amount of sediment in the region (mean thickness, 3.4 m). The lack of sediment primarily reflects decreased accommodation space (note shallower depth contours on Maps A, C) and limited sediment supply; (4) The Point Reyes bar domain, located west and south of the Point Reyes headland, is a local zone of increased sediment thickness (mean thickness, 14.3 m) created by bar deposition on the more protected south flank of the Point Reyes headland during rising sea level; (5) The Holomas shelf domain, located east and southeast of the Point Reyes headland (including most of the Drakes Bay and vicinity map area), has a thin sediment cover (mean thickness, 5.6 m), which likely reflects limited sediment accommodation space caused by tectonic uplift (water depths in this domain within California's State Waters are less than 45 m), as well as the limited sediment supply and the high wave energy capable of reworking and transporting shelf sediment to deeper water.

Map E shows the regional pattern of major faults and of earthquakes occurring between 1967 and 2014 that have inferred or measured magnitudes of 2.0 and greater. Fault locations, which have been simplified, are compiled from our mapping within California's State Waters (see sheet 10), from McCulloch (1987), and from the U.S. Geological Survey's Quaternary fault and fold database (U.S. Geological Survey and California Geological Survey, 2010). Earthquake epicenters are from the Northern California Earthquake Data Center (2014), which is maintained by the U.S. Geological Survey and the University of California, Berkeley, Seismological Laboratory. The largest earthquake in the map area (M2.4, 12/21/1998) was located within the broad San Andreas Fault zone north of Bodega Head. A notable lack of microseismicity on the San Andreas Fault in this region has occurred since the devastating great 1906 California earthquake (M7.8, 4/18/1906), thought to have nucleated on the San Andreas Fault offshore of San Francisco (see, for example, Bolt, 1968; Lomax, 2005), about 70 km south of the map area, with the rupture extending northward through the map area to the south flank of Cape Mendocino.

REFERENCES CITED

Bolt, B.A., 1968. The focus of the 1906 California earthquake. *Bulletin of the Seismological Society of America*, v. 58, p. 457-471.

Demopoulos, S., 1991. Surface and near-surface variations from the continental shelf of the Russian River, northern California. *Marine Geology*, v. 99, p. 163-173.

Drake, D.E., and Cacchione, D.A., 1985. Seasonal variation in sediment transport on the Russian River shelf, California. *Continental Shelf Research*, v. 4, p. 495-514. doi:10.1016/0278-4343(85)90007-X.

Farnsworth, K.L., and Warrick, J.A., 2007. Sources, dispersal, and fate of fine sediment supplied to coastal California. U.S. Geological Survey Scientific Investigations Report 2007-5254, 77 p., available at <http://pubs.usgs.gov/of/2007/5254/>.

Lomax, A., 2005. A reanalysis of the hypocentral location and related observations for the Great 1906 California earthquake. *Bulletin of the Seismological Society of America*, v. 95, p. 881-877. doi:10.1785/BSSA0404.1.

McCulloch, D.S., 1987. Regional geology and hydrocarbon potential of offshore central California. In Scholl, D.W., Grantz, A., and Vedder, J.G., eds., *Geology and resource potential of the continental margin of western North America and adjacent ocean basins—Beaufort Sea to Baja California*. Circum-Pacific Council for Energy and Mineral Resources, Earth Sciences Series, v. 3, p. 355-401.

Mitchum, R.M., Jr., Vail, P.R., and Sangree, J.B., 1977. Seismic stratigraphy and global changes of sea level, part 6—Stratigraphic interpretation of seismic reflection patterns in depositional sequences. In Payton, C.E., ed., *Seismic stratigraphy—Applications to hydrocarbon exploration*. Tulsa, Okla., American Association of Petroleum Geologists, p. 117-133.

Northern California Earthquake Data Center, 2014. Northern California earthquake catalog: Northern California Earthquake Data Center database, accessed April 5, 2014, at <http://www.nceq.org/ncsc/>.

Potter, W.R., and Fairbanks, R.G., 2006. Global glacial ice volume and Last Glacial Maximum duration from an extended Barbados sea level record. *Quaternary Science Reviews*, v. 25, p. 3322-3337. doi:10.1016/j.quascirev.2006.04.010.

Stanford, J.D., Hemmingsway, R., Rohling, E.J., Challenor, P.G., Medina-Elizalde, M., and Lister, A.J., 2011. Sea-level probability for the last deglaciation—A statistical analysis of ice-sheet records. *Global and Planetary Change*, v. 79, p. 195-201. doi:10.1016/j.gloplacha.2010.11.002.

U.S. Geological Survey and California Geological Survey, 2010. Quaternary fault and fold database of the United States. U.S. Geological Survey database, accessed April 5, 2014, at <http://earthquake.usgs.gov/quaternary-faults/>.

Wong, F.L., Phillips, E.L., Johnson, S.V., and Slinger, W., 2012. Modeling of depth to base of Last Glacial Maximum and sea-level sediment thickness for the California State Waters Map Series, eastern Santa Barbara Channel, California. U.S. Geological Survey Open-File Report 2012-1161, 16 p., available at <http://pubs.usgs.gov/of/2012/1161/>.

REFERENCES CITED

Bolt, B.A., 1968. The focus of the 1906 California earthquake. *Bulletin of the Seismological Society of America*, v. 58, p. 457-471.

Demopoulos, S., 1991. Surface and near-surface variations from the continental shelf of the Russian River, northern California. *Marine Geology*, v. 99, p. 163-173.

Drake, D.E., and Cacchione, D.A., 1985. Seasonal variation in sediment transport on the Russian River shelf, California. *Continental Shelf Research*, v. 4, p. 495-514. doi:10.1016/0278-4343(85)90007-X.

Farnsworth, K.L., and Warrick, J.A., 2007. Sources, dispersal, and fate of fine sediment supplied to coastal California. U.S. Geological Survey Scientific Investigations Report 2007-5254, 77 p., available at <http://pubs.usgs.gov/of/2007/5254/>.

Lomax, A., 2005. A reanalysis of the hypocentral location and related observations for the Great 1906 California earthquake. *Bulletin of the Seismological Society of America*, v. 95, p. 881-877. doi:10.1785/BSSA0404.1.

McCulloch, D.S., 1987. Regional geology and hydrocarbon potential of offshore central California. In Scholl, D.W., Grantz, A., and Vedder, J.G., eds., *Geology and resource potential of the continental margin of western North America and adjacent ocean basins—Beaufort Sea to Baja California*. Circum-Pacific Council for Energy and Mineral Resources, Earth Sciences Series, v. 3, p. 355-401.

Mitchum, R.M., Jr., Vail, P.R., and Sangree, J.B., 1977. Seismic stratigraphy and global changes of sea level, part 6—Stratigraphic interpretation of seismic reflection patterns in depositional sequences. In Payton, C.E., ed., *Seismic stratigraphy—Applications to hydrocarbon exploration*. Tulsa, Okla., American Association of Petroleum Geologists, p. 117-133.

Northern California Earthquake Data Center, 2014. Northern California earthquake catalog: Northern California Earthquake Data Center database, accessed April 5, 2014, at <http://www.nceq.org/ncsc/>.

Potter, W.R., and Fairbanks, R.G., 2006. Global glacial ice volume and Last Glacial Maximum duration from an extended Barbados sea level record. *Quaternary Science Reviews*, v. 25, p. 3322-3337. doi:10.1016/j.quascirev.2006.04.010.

Stanford, J.D., Hemmingsway, R., Rohling, E.J., Challenor, P.G., Medina-Elizalde, M., and Lister, A.J., 2011. Sea-level probability for the last deglaciation—A statistical analysis of ice-sheet records. *Global and Planetary Change*, v. 79, p. 195-201. doi:10.1016/j.gloplacha.2010.11.002.

U.S. Geological Survey and California Geological Survey, 2010. Quaternary fault and fold database of the United States. U.S. Geological Survey database, accessed April 5, 2014, at <http://earthquake.usgs.gov/quaternary-faults/>.

Wong, F.L., Phillips, E.L., Johnson, S.V., and Slinger, W., 2012. Modeling of depth to base of Last Glacial Maximum and sea-level sediment thickness for the California State Waters Map Series, eastern Santa Barbara Channel, California. U.S. Geological Survey Open-File Report 2012-1161, 16 p., available at <http://pubs.usgs.gov/of/2012/1161/>.